HHS Public Access

Author manuscript

Cell Rep. Author manuscript; available in PMC 2020 December 09.

Published in final edited form as:

Cell Rep. 2020 November 24; 33(8): 108430. doi:10.1016/j.celrep.2020.108430.

Antibody Isotype Switching as a Mechanism to Counter HIV Neutralization Escape

Cathrine Scheepers[1,2], **Valerie Bekker**[1], **Colin Anthony**[3], **Simone I. Richardson**[1,2], **Brent Oosthuysen**[1], **Thandeka Moyo**[1,2], **Prudence Kgagudi**[1], **Dale Kitchin**[1,2], **Molati Nonyane**[1], **Talita York**[3], **Dieter Mielke**[3], **Batsirai M. Mabvakure**[1,2,8], **Zizhang Sheng**[4,5], **Bronwen E. Lambson**[1,2], **Arshad Ismail**[1], **Nigel J. Garrett**[6], **Salim S. Abdool Karim**[6,7], **Lawrence Shapiro**[4,5], **Carolyn Williamson**[3], **Lynn Morris**[1,2,6,*], **Penny L. Moore**[1,2,3,6,9,*]

[1]Centre for HIV and STIs, National Institute for Communicable Diseases of the National Health Laboratory Service, Johannesburg 2131, South Africa

[2]Antibody Immunity Research Unit, School of Pathology, University of the Witwatersrand, Johannesburg 2050, South Africa

[3]Institute of Infectious Disease and Molecular Medicine, University of Cape Town, Cape Town 7701, South Africa

[4]Department of Biochemistry and Molecular Biophysics, Columbia University, New York, NY 10032, USA

[5]Zuckerman Brain Mind Behaviour Institute, Columbia University, New York, NY 10027, USA

[6]Centre for the AIDS Programme of Research in South Africa (CAPRISA), KwaZulu-Natal 4013, South Africa

[7]Department of Epidemiology, Columbia University, New York, NY 10032, USA

[8]Present address: Department of Pathology, Johns Hopkins University, School of Medicine, Baltimore, MD 21205, USA

[9]Lead Contact

SUMMARY

*Correspondence: lynnm@nicd.ac.za (L.M.), pennym@nicd.ac.za (P.L.M.).

AUTHOR CONTRIBUTIONS

C. S. designed and conducted experiments, analyzed the data, and wrote the manuscript; V.B. conducted antibody-neutralization assays and designed the experiments; C.A. analyzed viral NGS data; S.I.R. conducted ADCC experiments; B.O. and B.E.L. cloned and expressed antibodies; T.M. conducted antibody-binding assays; P.K. conducted antibody-neutralization assays and grew viruses; T.Y. and D.M. conducted viral NGS experiments; D.K. and M.N. conducted viral single-genome amplification (SGA) sequencing; B.M.M. and Z.S. analyzed antibody NGS data; A.I. designed and conducted antibody MiSeq experiments; N.J.G. and S.S.A.K. provided clinical samples; L.S. provided supervision on the antibody NGS analysis; C.W. provided supervision on the viral NGS sequencing and analysis; and L.M. and P.L.M. provided guidance on experimental design and data analysis and wrote the manuscript. All authors commented on the manuscript.

SUPPLEMENTAL INFORMATION

Supplemental Information can be found online at https://doi.org/10.1016/j.celrep.2020.108430.

DECLARATION OF INTERESTS

The authors declare no competing interests.

Neutralizing antibodies (nAbs) to highly variable viral pathogens show remarkable diversification during infection, resulting in an “arms race” between virus and host. Studies of nAb lineages have shown how somatic hypermutation (SHM) in immunoglobulin (Ig)-variable regions enables maturing antibodies to neutralize emerging viral escape variants. However, the Ig-constant region (which determines isotype) can also influence epitope recognition. Here, we use longitudinal deep sequencing of an HIV-directed nAb lineage, CAP88-CH06, and identify several co-circulating isotypes (IgG3, IgG1, IgA1, IgG2, and IgA2), some of which share identical variable regions. First, we show that IgG3 and IgA1 isotypes are better able to neutralize longitudinal autologous viruses and epitope mutants than can IgG1. Second, detrimental class-switch recombination (CSR) events that resulted in reduced neutralization can be rescued by further CSR, which we term “switch redemption.” Thus, CSR represents an additional immunological mechanism to counter viral escape from HIV-specific antibody responses.

Graphical Abstract

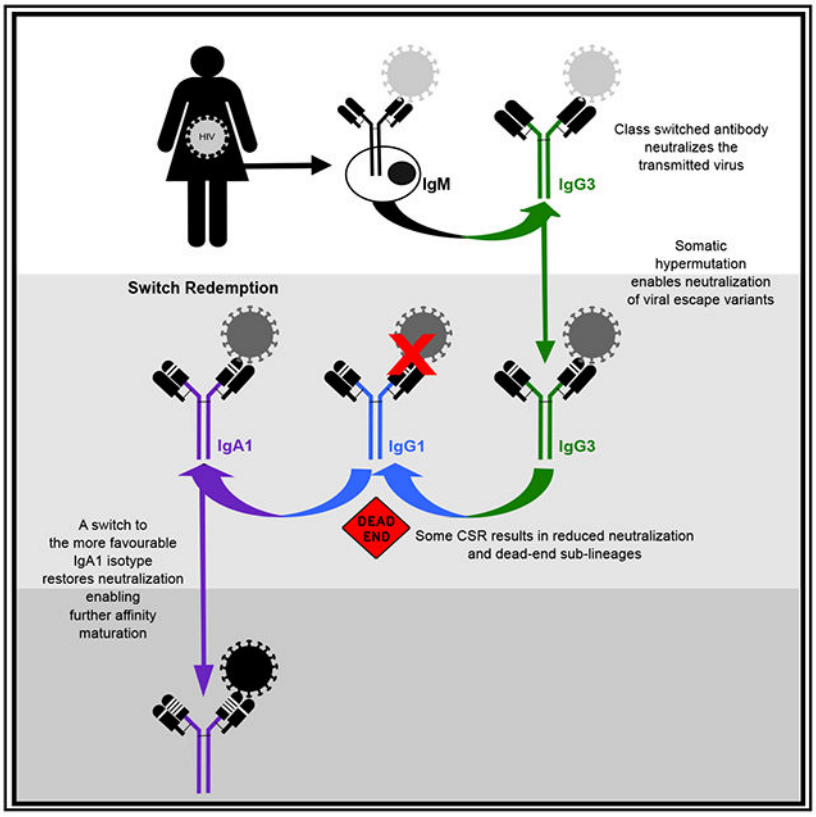

In Brief

Scheepers et al. show within an HIV-specific antibody lineage that isotypes confer variable ability to neutralize emerging viral escape variants. This suggests that class switching, in addition to somatic hypermutation of immunoglobulin-variable regions, contributes to antibody maturation during infection.

INTRODUCTION

Antibodies are key components of the adaptive immune response that act directly through Fab-mediated binding and neutralization. The role of somatic hypermutation (SHM) in the maturation of HIV-directed neutralizing antibody (nAb) lineages has been extremely well characterized, with the accumulation of mutations in variable regions conferring increased neutralization capacity (Bhiman et al., 2015; Doria-Rose et al., 2014; Liao et al., 2013; Soto et al., 2016; Wu et al., 2015). However, antibody diversification during infection is also achieved through class-switch recombination (CSR), which allows the expression of antibodies as one of five isotypes that differentially engage innate effector cells through binding to Fc receptors (Schroeder and Cavacini, 2010). Furthermore, isotypes can directly affect neutralization potency of engineered monoclonal antibodies (Kozel et al., 2007; Maurer et al., 2018; Richardson et al., 2019; Tudor et al., 2012), and the Fc region may contribute to viral escape (Horwitz et al., 2017). Recently, the identification of both immunoglobulin (Ig) G and IgA members of HIV-directed antibody lineages has further highlighted intra-lineage isotype variation (Jia et al., 2020). A key question, however, is whether CSR contributes to the maturation of natural antibody lineages during the course of viral infection.

RESULTS

We previously described an HIV-1 subtype-C-infected donor, CAP88, who developed potent neutralizing antibodies against the C3 region of the HIV envelope (Env), which drove rapid viral escape (Moore et al., 2009). The isolation of a C3-directed IgA1 monoclonal antibody (mAb), CAP88-CH06 (Gray et al., 2011), prompted us to explore the role of CSR in antibody-virus co-evolution in that donor. Longitudinal next-generation sequencing (NGS) of peripheral blood mononuclear cells (PBMCs) at multiple times identified clonal relatives of CAP88-CH06 (Figure 1A; Table S1), including multiple co-circulating isotypes comprising IgG3, IgG1, IgA1, IgG2, and IgA2 (Figure 1B). Average SHM increased until 46 weeks post infection (wpi), consistent with plasma neutralization titers, whereas, at 108 wpi, we detected only a single less mutated sequence, identical to one from 34 wpi and, thus, presumably persisting from an earlier time point (Figure 1A). SHM was greater in the heavy chain compared with the light chain (Figure 1A), suggesting that the heavy chain was the major contributor to neutralization, which we confirmed experimentally (Figure S2).

Analysis of heavy chain sequences revealed temporal variation of isotypes, with IgG1 predominant at 11 wpi, IgG3 at 17–38 wpi, and IgA1 at 46 and 108 wpi (Figure 1B). IgG2 and IgA2 were rarely observed, although both were detected at 11 wpi, and IgA2 was also present at 34 wpi. All isotypes showed increasing SHM reaching levels between 8% and 11% by 46 wpi (Figure 1C). A single sequence with no SHM in the V and J genes, but mutations in the D region through “N” additions/SHM (Figures S1A and S1B), was detected in the NGS data as either an IgG1 or IgG3 at 8 wpi and represents the last common ancestor (LCA) of this lineage. The relative position of the *IGHC* genes, responsible for encoding isotypes on chromosome 14, and the irreversible nature of gene excision during CSR enabled the determination of directionality for isotype switches within the lineage (Figure 1D). The existence of mature IgG3 lineage members (Figure 1E) indicated that the LCA

must have occurred as an IgG3. A large proportion of the lineage continued to mature as IgG3; however, we also observed identical antibody-variable regions expressed as different isotypes (Figures 1E and S1C). One sequence (H1) must also have existed as IgG3 because it gave rise to IgG3 ancestors but was only observed as IgG1, IgG2, IgA1, and IgA2 in the NGS data (Figure 1E). The more mature H7 and H8 sequences were observed as both IgG1 and IgG3. The topology of the tree suggests that CSR events were largely sequential from IgM to IgG3, then IgG1 and, in some minor branches, to IgA1 (with one IgA1 branch ultimately resulting in CAP88-CH06). In addition, the accumulation of SHM between class switches varied, with IgG3 to IgG1 generally associated with few mutations (<5). In contrast, switches from IgG1 to IgA1 were associated with high levels of SHM (12–16), likely occurring within germinal centers (GCs) (Figure 1E). Overall, these data are consistent with previous reports of antibodies with identical variable regions but different isotypes in response to infections by other pathogens (Janda et al., 2016) and autoimmunity and, in healthy individuals, indicative of B cell clones having undergone multiple class-switch events (Petrova et al., 2018).

To assess the role of isotype in antibody-virus co-evolution, we selected nine heavy-chain sequences with varying levels of SHM (Figure 1E, H1–H9) and expressed these with the CAP88-CH06 light chain (Figures 2A and S1A). Identical antibodies that occurred as multiple isotypes were cloned and expressed in these forms. In addition, the LCA and CAP88-CH06 (which was isolated as IgA1) were expressed as IgG1, IgG3, and IgA1 for cross-isotype comparison. Antibodies were tested in an Env-pseudotyped neutralization assay against single-genome-derived, autologous Envs from viruses circulating during the first year of infection (Figures 2A and S3A). The LCA potently neutralized the transmitted/founder (T/F) virus from 5 wpi, similar to our previous observation of neutralization by an HIV-directed LCA (Doria-Rose et al., 2014). Furthermore, as expected, higher levels of SHM were associated with improved neutralization potency against the T/F virus, and an increased ability to neutralize viruses from later time points. However, no mAbs neutralized viruses from 57 wpi, consistent with the emergence of escape mutations (Figure S3B). These data confirmed that SHM contributed to antibody maturation, until viral escape precluded further neutralization.

Interestingly, we also observed differences in neutralization and binding of autologous viruses, based on the isotype of the antibody (Figures 2 and S4A). The LCA was more potent as an IgG3, whereas the mature CAP88-CH06 was more potent as an IgA1 (Figure 2B). In all instances, IgG3 and IgA1 showed better neutralization of autologous viruses, both in terms of potency and the number of viruses neutralized, compared with IgG1, with these differences reaching statistical significance for CAP88-CH06, H7, and H8 (Figure 2C). Similarly, CAP88-CH06 expressed as IgA1 and IgG3 showed better binding (K_D = 2.01 and 1.54, respectively) than IgG1 (K_D = 3.69) when tested against a gp120 that was derived from a 30-wpi virus with significantly different neutralization sensitivity (Figure S4A). This difference was not attributable solely to IgG3 antibody aggregation (Figure S4B). Because isotype differentially modulates effector function (Schroeder and Cavacini, 2010), we also showed that the LCA and CAP88-CH06 expressed as IgG3 mediated the increased antibody-dependent cellular cytotoxicity (ADCC) against the CAP88 T/F virus compared with IgG1 or IgA1 versions, consistent with other studies (Damelang et al., 2019) (Figure S4C).

Overall, these data indicated that antibody isotype, in addition to affecting the Fc effector function, can improve the ability of antibodies to bind and neutralize emerging viral variants.

Mutations able to mediate viral escape from CAP88-CH06 (Gray et al., 2011) were quantified by deep sequencing of the CAP88 plasma virus during the first year of infection (Table S2). Significant toggling occurred at residues 339, 343, 350, and 358, located within or proximal to the solvent-exposed alpha-2 helix of C3. The most common and sustained escape mutations were I339N (introducing a glycan sequon), E343K, E350K, and a single amino acid (aa) deletion (K358del). The E343K and E350K mutations peaked between 13 and 15 wpi and, thereafter, occurred with I339N, which became fixed in the population (Figure 3A). The combination of I339N and either E350K or K358del, with or without other escape mutations, accounted for more than 90% of the viruses from 38 wpi. Introduction of escape mutations into the CAP88 T/F virus was performed to assess their effect on neutralization by antibodies of different isotypes (Figure 3B). Similar to longitudinal viruses, increased SHM conferred improved neutralization of viruses bearing escape mutations, with early mAbs neutralizing fewer mutants than more-mature antibodies (Figure 3B; Table S3). Viral mutations were associated with varying levels of neutralization resistance, with E343K conferring resistance to early mAbs (<11wpi), and I339N and I339N +E343K introducing resistance to mAbs isolated up to 34 wpi. However, even the most mature mAbs failed to neutralize viruses containing the K358del and I339N+E350K mutations, accounting for the lack of antibody maturation after 46 wpi (Figure 1A).

We also observed differential neutralization of escape variants between isotypes. For example, CAP88-CH06 expressed as IgG3 or IgA1 showed better neutralization of viruses containing E343K, I339N, and I339N+E343K than the matched IgG1 version did (Figure 3C). Overall, for CAP88-CH06, H7, and H8, the IgG1 versions were significantly less effective at neutralizing viral escape variants than otherwise identical antibodies (Figure 3D). These data show that isotype, in addition to SHM, influenced the neutralization of viruses containing escape mutations.

Our data suggest that isotype switching may have either beneficial or deleterious outcomes for antibody evolution. In this lineage, early switches from H1-IgG3 to IgG1, IgA1, or IgA2 resulted in “dead-end” sub-lineages that are unable to neutralize the early E343K viral escape variant that was neutralized by the LCA-IgG3 and H1-IgG3 (Figure 4). The selection of IgG3 clones better able to neutralize emerging viral variants fostered continued maturation of the lineage. However, again, detrimental switches from IgG3 to IgG1 (H7 and H8) resulted in reduced neutralization of viruses with escape mutations. In contrast, the emergence of IgA1 sub-lineages from IgG1 dead-end precursors (Figure 1E) suggests that switching to IgA1 restored the ability of antibodies to neutralize emerging viruses bearing escape mutations. This “switch redemption” is illustrated using CAP88-CH06, where an initial switch from an IgG3 to IgG1 resulted in reduced neutralization of the E343K and I339N mutants and loss of neutralization of I339N+E343K. Neutralization was restored by a further switch to an IgA1, which enhanced neutralization of E343K or I339N mutants and restored the ability of antibodies to neutralize viruses bearing I339N+E343K. This switch redemption thereby enabled further maturation of the IgA1 sub-lineage, with H9 showing increased SHM and enhanced neutralization potency against the same viruses (Figure 4).

DISCUSSION

In conclusion, we have shown that isotype switching, in addition to SHM, contributes to antibody-virus co-evolution by conferring differential neutralization of emerging viral variants. Although several studies of individual mAbs have shown that isotype can affect neutralizing activity (Jia et al., 2020; Kozel et al., 2007; Maurer et al., 2018; Richardson et al., 2019; Tudor et al., 2012), this is the first, to our knowledge, to systematically evaluate the contribution of CSR to the evolution of a nAb lineage. The combined role of both SHM and CSR in adjusting B cell specificity has been well described in the intestinal mucosa, where continuous exposure to commensal microbiota results in iterative "editing" of IgM/IgA specificities in response to the changing microbiota (Benckert et al., 2011; Ellebrecht et al., 2018; He et al., 2007; Horns et al., 2016; Kawamoto et al., 2014; Kitaura et al., 2017; Lindner et al., 2015; Magri et al., 2017; Planer et al., 2016). This is analogous to what we have shown here, with continuous exposure to a changing viral quasispecies similarly driving Env-reactive B cells to "adjust" their variable and constant domains through SHM and CSR.

The CAP88-CH06 antibody lineage was sequenced from PBMCs and sequences were thus most likely from plasma and memory B cells, although their specific origin could not be determined. The identification of IgA1 and IgA2, enriched at mucosal surfaces, raises the possibility that these antibodies may be derived from gut-homing memory B cells (He et al., 2007). However, although IgA1/2 exist predominantly as dimers at mucosal surfaces, these antibodies are mostly monomeric in plasma (80%–99%), enabling us to directly compare the neutralization of IgA1 monomers with IgG1/IgG3 in this study (Schroeder and Cavacini, 2010; Woof and Mestecky, 2005).

CSR can occur both sequentially from IgM through IgG, then to IgA, or directly from IgM to IgA through the deletion of intermediate genes. Much of the CAP88 lineage persists as IgG3; however, we also observed sequential CSR in sub-lineages from the LCA-IgG3 to IgG1, followed by IgA1. Our data are consistent with both with reports of preferential switching to IgG3 during early HIV-1 infection (Kardava and Moir, 2019; Yates et al., 2011) and with previous studies of CSR frequency in which IgG3 B cells most frequently switch to IgG1/IgG2 (~87%) and IgG1 to IgA1/IgG2 (92%) (Horns et al., 2016; Jackson et al., 2014). Our sequencing has certainly not fully captured the total level of isotype variation within this lineage, as indicated by the fact that we did not detect the H1-IgG3 transcript. Despite that, we show that class switching has important functional consequences for lineage maturation.

It has become increasingly evident that SHM can have either advantageous or disadvantageous effects on neutralization (Pappas et al., 2014; Sacks et al., 2019). Here, we show, likewise, that CSR can have variable outcomes for neutralization. We provide evidence that disadvantageous class switches can be redeemed by a further stochastic switch resulting in antibodies with increased neutralization, which we term "switch redemption." The persistence and progeny of isotypes with enhanced neutralization indicates that, within germinal centers, these B cells were preferentially selected for (Victora and Nussenzweig, 2012). This concept of switch redemption is, in some respects, similar to that of "clonal

redemption" of auto-reactive nAbs by SHM (Finney and Kelsoe, 2018; Reed et al., 2016; Sabouri et al., 2014).

The effect of Fc on epitope recognition is influenced by structural differences among antibody isotypes (Giuntini et al., 2016; Janda et al., 2016; Schroeder and Cavacini, 2010). IgG3 has the longest hinge (up to 62 aa), which can enhance neutralization (Richardson et al., 2019; Vidarsson et al., 2014). Although IgA1 has a similar hinge length to IgG1 (~17–18 aa), it typically has a more open conformation, is highly glycosylated, and has a distinct CH1 that has been linked to improved viral neutralization (Maurer et al., 2018; Miranda et al., 2007; Tudor et al., 2012; Woof and Mestecky, 2005; Woof and Russell, 2011). Together these features likely provide a mechanism for the enhanced neutralization of IgG3 and IgA1 versions of CAP88-CH06 lineage antibodies compared with IgG1. However, many HIV antibodies isolated as IgG1 have high levels of neutralization breadth and potency (Kwong and Mascola, 2018), and IgA and IgG3 have been associated with divergent outcomes in vaccine trials and transmission experiments (Astronomo et al., 2016; Kulkarni and Ruprecht, 2017; Neidich et al., 2019). Thus, the influence of isotype on neutralization almost certainly varies between and within lineages.

Nonetheless, our data indicate that previous co-evolution studies, which have used IgG1-expressed antibodies, regardless of the native isotype, may not completely capture the diversity of antibody maturation pathways. Furthermore, because isotype diversity correlates with neutralization breadth (Richardson et al., 2018), these data have translational implications for vaccines to HIV and other pathogens, highlighting the need for adjuvants that drive both SHM and isotype diversity (Avramidis et al., 2002; Knudsen et al., 2016). Overall, these data add a new layer of complexity to our understanding of nAb maturation.

Limitations of Study

Here, we measured the relationship between antibody and antigen by functional neutralization assays and, in a smaller subset, by binding to soluble antigens. Follow-up studies will need to provide a mechanistic explanation for the varying effect of isotype on binding and neutralization in the context of otherwise identical antibodies. In addition, such studies will need to interrogate the relationship between binding, neutralization, and B cell receptor activation, a more sensitive proxy of B cell selection in germinal centers. These data will further define the role of switch redemption in antibody lineage maturation.

STAR★METHODS

RESOURCE AVAILABILITY

Lead Contact—Further information and requests for resources and reagents should be directed to and will be fulfilled by the Lead Contact, Penny Moore (pennym@nicd.ac.za).

Materials Availability—This study did not generate new unique materials.

Data and Code Availability—Unprocessed MiSeq antibody sequencing data for the CAP88-CH06 lineage, and viral C3 deep sequencing, have been deposited for public access into the National Center for Biotechnology Information (NCBI) Sequence Read Archive

(SRA), under the following Bio-Project accession numbers: SRA:PRJNA556126 and SRA:PRJNA557574. The heavy and light chain antibody sequences used to generate the LCA and CAP88-CH06 as well as heavy chains of H1 – H9 have been deposited into GenBank, and their accession numbers are listed in the Key Resources Table. Viral envelope sequences are also available in GenBank, accession numbers provided in the Key Resources Table.

Custom data analysis pipelines used for viral NGS analysis are available on GitHub (links provided in the Key Resources Table).

EXPERIMENTAL MODELS AND SUBJECT DETAILS

Human Subjects—CAP88, a CAPRISA 002 cohort participant, was infected with an HIV-1 subtype C virus in 2005 (Gray et al., 2007; van Loggerenberg et al., 2008). Stored plasma and peripheral blood mononuclear cells (PBMCs) from 5 - 108 weeks post-infection were used for virus gp160 envelope cloning and for antibody studies. The CAPRISA 002 study was approved by the ethics committees of the University of KwaZulu-Natal (E013/04), the University of Cape Town (025/2004) and the University of the Witwatersrand (MM040202) and included informed consent from donor CAP88.

Cell Lines—HEK293F suspension cells were cultured in 293Freestyle media (GIBCO) and grown in a shaking incubator at 37°C, 5% CO2, 70% humidity at 125rpm. HEK293T cells were obtained from Dr. George Shaw (University of Alabama, Birmingham, AL) and were used for the expression of proviral IMC plasmid DNA for ADCC assays. These adherent cell lines were cultured at 37°C, 5% CO2, in DMEM containing 10% heat-inactivated fetal bovine serum (GIBCO) and supplemented with 50 μg/ml gentamicin (Sigma). Cells were disrupted at confluence with 0.25% trypsin in 1 m MEDTA (Sigma) every 48–72 hours. CEM-NK^{R}_{CCR5} were obtained from the AIDS Reagent Program (Division of AIDS, NIAID, NIH) and used as target cells in the ADCC assay. These cells were cultured at 37°C, 5% CO2 in RPMI containing 10% heat-inactivated fetal bovine serum (GIBCO) and 1% Penicillin Streptomycin (GIBCO). TZM-bl cells (JC53-bl (clone 13)) cells were obtained from AIDS Reagent Program (Division of AIDS, NIAID, NIH) and used for the neutralization assays (Montefiori, 2005).

METHOD DETAILS

CAP88-CH06 lineage next generation sequencing—Total RNA was extracted from cryopreserved PBMC at 7 different time-points (8, 11, 17, 34, 38, 46 and 108 wpi) using the AllPrep DNA/RNA mini kit (QIAGEN). Reverse transcription was carried out using Random Hexamers (Integrated DNA Technologies) and Superscript III RT enzyme (Invitrogen). Lineage specific primers bound leader regions of *IGHV4-39* and *IGLV3-21* and included the Illumina MiSeq barcodes to allow sequencing on the MiSeq (primers listed in the Key Resources Table). Samples from each time point were amplified as seven replicates for both the heavy and light chains, to ensure adequate coverage and to minimize PCR bias. PCR conditions were based on previous experiments (Scheepers et al., 2015) but modified by increasing the annealing temperature to 65°C and reducing cycles to 25. Nextera XT unique dual indexing combinations selected from Illumina Indexing Kit V2 Set

B were added to the pooled MiSeq amplicon libraries. All products were checked on an Agilent Bioanalyser High Sensitivity DNA kit (Diagnostech) and Qubit dsDNA HS assay (ThermoFischer Scientific) and cleaned-up using 0.75X Ampure Beads (Beckman-Coulter). A final concentration of 4.5 pM denatured DNA library with 10% PhiX control (Illumina) was run on the Illumina MiSeq, using the MiSeq reagent kit (version 3) with 2 × 300 paired-end reads.

CAP88-CH06 lineage analysis—Paired-end MiSeq reads were merged into full-length reads for each time point using PEAR (Zhang et al., 2014). Paired sequences were then de-replicated using USEARCH (Edgar, 2010) resulting in unique reads. The SONAR bioinformatics pipeline (Schramm et al., 2016) was used to identify CAP88-CH06 clonally related reads. In brief, germline V and J genes were assigned, the CDR3 regions were identified, and identity to CAP88-CH06 for each of the reads was calculated. Clonally related sequences were selected based on germline gene usage and CDR3 identity ≥ 90% to CAP88-CH06. To account for sequencing and/or PCR error, all singletons were removed and the remaining sequences were clustered at 99% identity using USEARCH, and the most abundant representative was selected from clusters with three or more transcripts for downstream analyses. Tools from the immcantation portal were used to reconstruct the antibody lineage and create the phylogenetic tree (Gupta et al., 2015). Briefly, clonally related heavy chain sequences were submitted to IMGT High V-quest (Alamyar et al., 2012; Li et al., 2013) for analysis and the resulting summary files were then parsed into a Change-O database. The LCA of the lineage was used as the germline defined sequence for the reconstruction. Within R, the Alakazam package (Stern et al., 2014) was used to read in the Change-O database and reconstruct the lineage creating clones and introducing inferred sequences using buildPhylipLineage. The resulting tree was plotted using igraph (Csardi and Nepusz, 2006). The edge lengths of the tree were further modified to be proportional to the number of mutations between nodes and all nodes with no mutations from the parent node were deleted using Inkscape v 0.91.

CAP88-CH06 lineage antibody production—Selected clonally related heavy and light chain sequences were ordered from GenScript. All heavy chain clonally related sequences were paired with the mature CAP88-CH06 light chain. The LCA heavy chain was paired with the LCA light chain (LCA). These heavy and light chain pairs were sub-cloned into IgG1, IgG3, IgA1 or IgA2 backbones, co-transfected and expressed in HEK293F cells (NIH AIDS Reagent Program), confirmed to be *Mycoplasma* free, grown in FreeStyle 293 Expression Medium (GIBCO) at 37°C, 5% CO2, 70% humidity and 125 rpm. Cultures were harvested after seven days by centrifugation at 4000 x g, and supernatants were filtered through a 0.22 μm filter. Filtered supernatant of IgG1, IgG3, IgA1 and IgA2 antibodies were purified by chromatography using protein A-Agarose (BioVision), immobilized protein G (ThermoFischer Scientific) and CaptureSelect™ IgA affinity matrix (ThermoFischer Scientific), respectively.

Size exclusion chromatography—The different isotypes of CAP88-CH06 and LCA were analyzed using size exclusion chromatography (SEC) on a Superdex 200 HiLoad 16/600 pg column (GE healthcare). The mAbs were run on the column equilibrated with 1x

phosphate buffered saline (PBS). All mAbs were run at a concentration of 1 mg/mL and volume of 1mL, with the exception of the CAP88-CH06-IgG3 in which only 500uL was run at 1mg/mL. The calibration and operations of the system were set as per manufacturer's instructions. Graphs were produced in GraphPad Prism version 8.0.

Single genome envelope amplification and sequencing—HIV-1 RNA was purified from plasma using the QiAamp Viral RNA kit (QIAGEN), and reverse transcribed to cDNA using Superscript III Reverse Transcriptase (Invitrogen). The *env* genes were amplified from single cDNA copies (Keele et al., 2008) and amplicons were directly sequenced using the ABI PRISM Big Dye Terminator Cycle Sequencing Ready Reaction kit (Applied Biosystems) and resolved on an Applied Biosystems 3500xL Genetic Analyzer. The full-length *env* sequences were assembled and edited using Sequencher v.5.4.6 software (Gene Codes Corporation). Multiple sequence alignments were performed using Clustal X v1.83 and edited with BioEdit v7.2.5.

Envelope cloning and production of env-pseudotyped viruses—Selected viral amplicons were cloned into the expression vector pcDNA™ 3.1D/V5-His-TOPO (Invitrogen) by re-amplification of SGA first-round products using PfuUltra II Fusion HS DNA polymerase (Agilent) with the EnvM and EnvA primers (Gao et al., 1996). Env-pseudotyped viruses were obtained by co-transfecting the Env plasmid with $pSG3^{\Delta env}$ (NIH AIDS Reagent) using FuGENE transfection reagent (Roche) as previously described (Gray et al., 2007).

Neutralization assays—Neutralization was measured as a reduction in luciferase gene expression after a single round infection of TZM-bl cells (NIH AIDS Reagent Program), confirmed to be *Mycoplasma* free, with Env-pseudotyped viruses (Montefiori, 2005). Titers were calculated as the inhibitory concentration (IC_{50}) or reciprocal plasma/serum dilution (ID_{50}) causing 50% reduction of relative light units (RLU) with respect to the virus control wells (untreated virus). Reported neutralization titers are the average of three or more titers for any given virus/antibody combination.

Antibody-gp120 binding assay using biolayer interferometry—The binding affinities of CAP88-CH06 expressed as IgG3, IgG1 and IgA1 against a his-tagged gp120 core derived from the CAP88_3100_030wpi_29 virus were measured by biolayer interferometry (BLI) using the Octet Red system (Pall FortéBio). Ni-NTA biosensors were initially hydrated in 1x kinetics buffer (1x PBS, 0.002% Tween, 0.01% bovine serum albumin) and loaded with 10 μg/mL gp120 for 60 s. Biosensors were then transferred into wells containing 1x kinetics buffer to achieve a baseline before being transferred into wells containing 2-fold serial dilutions of the antibodies at starting dilutions of 500 nM. This association phase was subsequently followed by a dissociation step with 1x kinetics buffer. Analysis was performed using Octet software with a 1:1 fit model. Experiments were repeated in duplicates or triplicates, and values were averaged.

Infected cell ADCC assay—The HIV-1 reporter virus used in the ADCC assays was a replication-competent infectious molecular clone (IMC) designed to encode the T/F virus (CAP88_2000_005wpi_17, subtype C) *env* gene *in cis* within an isogenic backbone (NL-

LucR.T2A-ENV.ecto) that also expresses the Renilla luciferase reporter gene, and preserves all viral open reading frames (Edmonds et al., 2010; Li et al., 2005). Reporter virus stocks were generated by transfection of HEK293T cells (NIH AIDS Reagent Program) with proviral IMC plasmid DNA, and titered in CEM.NK^{R}_{CCR5} cells (NIH AIDS Reagent Program) for infectivity by p24 staining (Beckman-Coulter). All cell lines were confirmed to be *Mycoplasma* negative. The infected cell assay was used to measure ADCC activity as previously described (Pollara et al., 2014). Briefly, a CEM.NK^{R}_{CCR5} cell line (NIH AIDS Reagent Program) was used as targets for ADCC luciferase assays after infection with the HIV-1 IMCs listed above. The target cell line was infected with IMC using titered stock that generated more than 50% infected target cells after 72 hours of infection. The target cells were incubated with 5-fold serially diluted mAbs starting at 50 μg/mL. Cryopreserved peripheral blood mononuclear cells (PBMC) obtained from a HIV seronegative donor with a high-affinity 158V/V Fcg receptor IIIa phenotype were used as source of effector cells. After thawing, the cryopreserved PBMCs were rested overnight and used at an effector to target ratio of 30:1. The effector cells, target cells, and Ab dilutions were plated in white 96-well half area plates and incubated for 6 hours at 37°C in 5% CO_2. The final readout was the luminescence intensity (in relative light units) generated by the presence of residual intact target cells that have not been lysed by the effector population in the presence of any ADCC-mediating mAb. The percentage of killing was calculated using the formula:

$$\%\,killing = \frac{(RLU\ of\ Target\ and\ Effector\ well) - (RLU\ of\ test\ well)}{RLU\ of\ Target\ and\ Effector\ well} \times 100$$

In this analysis, the RLU of the target plus effector wells represents non-antibody background. The RSV-specific mAb Palivizumab (Medimmune; Synagis) and A32 (NIH AIDS Reagent Program) (to show correct conformation of the envelope) were used as negative controls and a polyclonal mixture of IgG from Clade C HIV infected individuals from the NIH AIDS Reagent Program. Data are represented as the area under the curve (AUC) of percentage specific killing over the serially diluted antibodies.

Viral deep sequencing library preparation—Preparation of viral amplicons for deep sequencing (RNA extraction, cDNA synthesis and subsequent amplification), was carried out as described previously (Jabara et al., 2011), with the following modifications: A minimum of 5,000 HIV-1 RNA copies were isolated from longitudinal plasma samples spanning two years of infection, using the QIAamp Viral RNA kit (QIAGEN). The cDNA synthesis primer (ENV_C3_cDNA_R) was designed to bind to the C3 region of the HIV-1 envelope gene (HXB2 gp160 amino acid position 368-374) and included a randomly assigned 15-mer tag (Primer ID method), to uniquely label each cDNA molecule and assist with phasing over the first cycles of the MiSeq sequencing run. This tag was preceded by a universal primer binding site to allow out-nested PCR amplification of cDNA templates (primers are listed in Key Resources Table). The amplification primer (forward: ENV_C2_Fwd and reverse: Univ_i7_Rev) was designed to bind to the end of the C2 region (HXB2 gp160 amino acid position 221-228) and contained a template-specific binding region, preceded by seven randomly assigned bases to assist with phasing during MiSeq (primers provided in Key Resources Table). In addition, PCR primers contained 5′

overhangs, introducing binding sites for the Nextera XT indexing primers (Illumina, CA). This allowed the amplification of the C2 to C3 region of the envelope spanning HXB2 gp160 amino acid positions 228 to 368. Nested PCR reactions were carried out using the Nextera XT indexing kit (version 2, Set A). After indexing, samples were purified using SPIRselect magnetic beads (Beckman Coulter, CA) with a 'sample volume to bead ratio' of 1:0.65, for the removal of < 300bp fragments. Samples were quantified using the Qubit dsDNA HS assay (ThermoFisher) and pooled in equimolar concentrations. The pooled library was cleaned again using the SPIRselect magnetic beads to ensure primer removal before the final library was submitted for sequencing on an Illumina MiSeq (version 3), using 2 × 300 paired-end chemistry.

Viral deep sequencing data analysis—Custom data analysis pipelines used for viral NGS analysis are available on GitHub (links provided in the Key Resources Table). Raw reads were processed using an NGS_processing_pipeline to automate all steps. Briefly, this pipeline processes through the following steps: raw reads were length and quality filtered, merged using PEAR (Zhang et al., 2014), and processed according to the Primer ID method (Jabara et al., 2011), including the removal of sequences resulting from offspring bins (Zhou et al., 2015), using MotifBinner2. Consensus sequences were further processed to remove sequences with degenerate bases, large deletions (> 50bp), any non-HIV contaminating sequences. Finally, the resulting sequences were codon aligned to HXB2 using MAFFT v7.427(Katoh and Standley, 2013). The resulting codon alignment was then manually curated to correct any alignment errors. The entire haplotype (positions 339, 343, 351 and 358) was considered when calculating the amino acid frequencies for each escape variant genotype.

QUANTIFICATION AND STATISTICAL ANALYSIS

Differences in potency between isotypes for the LCA, H1, H7, H8 and CAP88-CH06 were assessed using the Wilcoxon Signed-Rank Test (R coin package) and effect sizes were calculated based on the absolute value of Wilcoxon Signed-Rank Test z-scores divided by the square root of the number of viruses tested for both antibodies: effect size = abs(z-score)/sqrt(# viruses). The number of viruses per comparison for autologous viruses were as follows: n = 6, n = 4, n = 16, n = 26, n = 18 for the LCA, H1, H7, H8 and CAP88-CH06, respectively. The number of viruses per comparison for escape mutations were as follows: n = 8, n = 6, n = 16, n = 20, n = 18 for the LCA, H1, H7, H8 and CAP88-CH06, respectively. All statistical tests were calculated using R, version 3.5.3.

Supplementary Material

Refer to Web version on PubMed Central for supplementary material.

ACKNOWLEDGMENTS

We thank participant CAP88 of the CAPRISA 002 cohort, Natasha Samsunder, and the CAPRISA laboratory, as well as clinical staff involved in sample collection and processing. At the NICD, we thank Frances Ayres, Sharon Madzorera, Zanele Molaudzi, Don Mvududu, and Dr. Charissa Oosthuysen for producing CAP88 viruses, mutants, CAP88-CH06 lineage antibodies, and size-exclusion chromatography. Dr. Chaim Schramm provided advice on the analysis of the CAP88-CH06 antibody lineage using SONAR. We thank Dr. Larry Liao for providing plasmids for different Ig isotypes and Dr. Christina Ochsenbauer for the CAP88_2000_005wpi_17 (T/F) IMC. We thank Dr.

Edward Sturrock and Sylva Schwager at the University of Cape Town for the use of the Octet system. C.S. was supported by the Columbia University-Southern African Fogarty AIDS International Training and Research Program (AITRP) through the Fogarty International Center, National Institutes of Health (grant 5 D43 TW000231), and the National Institute of Allergy and Infectious Diseases of the National Institutes of Health under award U01AI136677. P.L.M. is supported by the South African Research Chairs Initiative of the Department of Science and Innovation (DSI) and the National Research Foundation (NRF) (grant 98341). CAPRISA is funded by the National Institute of Allergy and Infectious Diseases (NIAID), National Institutes of Health (NIH), and U.S. Department of Health and Human Services (grant AI51794). This project was supported by the Poliomyelitis Research Foundation (grant 16/23), a University of the Witwatersrand Health Sciences Faculty Research Council grant, the South African NRF/DSI Centre of Excellence in HIV Prevention, and the South African Medical Research Council (SAMRC).

REFERENCES

Alamyar E, Giudicelli V, Li S, Duroux P, and Lefranc MP (2012). IMGT/High V-quest: the IMGT® web portal for immunoglobulin (IG) or antibody and T cell receptor (TR) analysis from NGS high throughput and deep sequencing. Immunome Res. 8, 1–15.

Astronomo RD, Santra S, Ballweber-Fleming L, Westerberg KG, Mach L, Hensley-McBain T, Sutherland L, Mildenberg B, Morton G, Yates NL, et al. (2016). Neutralization takes precedence over IgG or IgA isotype-related functions in mucosal HIV-1 antibody-mediated protection. EBioMedicine 14, 97–111. [PubMed: 27919754]

Avramidis N, Victoratos P, Yiangou M, and Hadjipetrou-Kourounakis L (2002). Adjuvant regulation of cytokine profile and antibody isotype of immune responses to Mycoplasma agalactiae in mice. Vet. Microbiol 88, 325–338. [PubMed: 12220808]

Benckert J, Schmolka N, Kreschel C, Zoller MJ, Sturm A, Wiedenmann B, and Wardemann H (2011). The majority of intestinal IgA+ and IgG+ plasmablasts in the human gut are antigen-specific. J. Clin. Invest 121, 1946–1955. [PubMed: 21490392]

Bhiman JN, Anthony C, Doria-Rose NA, Karimanzira O, Schramm CA, Khoza T, Kitchin D, Botha G, Gorman J, Garrett NJ, et al. (2015). Viral variants that initiate and drive maturation of V1V2-directed HIV-1 broadly neutralizing antibodies. Nat. Med 21, 1332–1336. [PubMed: 26457756]

Csardi G, and Nepusz T (2006). The Igraph software package for complex network research. interjournal Complex Syst. 1695, 1–9.

Damelang T, Rogerson SJ, Kent SJ, and Chung AW (2019). Role of IgG3 in infectious diseases. Trends Immunol. 40, 197–211. [PubMed: 30745265]

Doria-Rose NA, Schramm CA, Gorman J, Moore PL, Bhiman JN, DeKosky BJ, Ernandes MJ, Georgiev IS, Kim HJ, Pancera M, et al.; NISC Comparative Sequencing Program (2014). Developmental pathway for potent V1V2-directed HIV-neutralizing antibodies. Nature 509, 55–62. [PubMed: 24590074]

Edgar RC (2010). Search and clustering orders of magnitude faster than BLAST. Bioinformatics 26, 2460–2461. [PubMed: 20709691]

Edmonds TG, Ding H, Yuan X, Wei Q, Smith KS, Conway JA, Wieczorek L, Brown B, Polonis V, West JT, et al. (2010). Replication competent molecular clones of HIV-1 expressing Renilla luciferase facilitate the analysis of antibody inhibition in PBMC. Virology 408, 1–13. [PubMed: 20863545]

Ellebrecht CT, Mukherjee EM, Zheng Q, Choi EJ, Reddy SG, Mao X, and Payne AS (2018). Autoreactive IgG and IgA B cells evolve through distinct subclass switch pathways in the autoimmune disease pemphigus vulgaris. Cell Rep. 24, 2370–2380. [PubMed: 30157430]

Finney J, and Kelsoe G (2018). Poly- and autoreactivity of HIV-1 bNAbs: implications for vaccine design. Retrovirology 15, 53. [PubMed: 30055635]

Gao F, Morrison SG, Robertson DL, Thornton CL, Craig S, Karlsson G, Sodroski J, Morgado M, Galvao-Castro B, von Briesen H, et al. (1996). Molecular cloning and analysis of functional envelope genes from human immunodeficiency virus type 1 sequence subtypes A through G. The WHO and NIAID Networks for HIV Isolation and Characterization. J. Virol 70, 1651–1667. [PubMed: 8627686]

Giuntini S, Granoff DM, Beernink PT, Ihle O, Bratlie D, and Michaelsen TE (2016). Human IgG1, IgG3, and IgG3 hinge-truncated mutants show different protection capabilities against

meningococci depending on the target antigen and epitope specificity. Clin. Vaccine Immunol 23, 698–706. [PubMed: 27307451]

Gray ES, Moore PL, Choge IA, Decker JM, Bibollet-Ruche F, Li H, Leseka N, Treurnicht F, Mlisana K, Shaw GM, et al.; CAPRISA 002 Study Team (2007). Neutralizing antibody responses in acute human immunodeficiency virus type 1 subtype C infection. J. Virol 81, 6187–6196. [PubMed: 17409164]

Gray ES, Moody MA, Wibmer CK, Chen X, Marshall D, Amos J, Moore PL, Foulger A, Yu J-S, Lambson B, et al. (2011). Isolation of a monoclonal antibody that targets the alpha-2 helix of gp120 and represents the initial autologous neutralizing-antibody response in an HIV-1 subtype C-infected individual. J. Virol 85, 7719–7729. [PubMed: 21613396]

Gupta NT, Vander Heiden JA, Uduman M, Gadala-Maria D, Yaari G, and Kleinstein SH (2015). Change-O: a toolkit for analyzing large-scale B cell immunoglobulin repertoire sequencing data. Bioinformatics 31, 3356–3358. [PubMed: 26069265]

Hall TA (1999). BIOEDIT: a user-friendly biological sequence alignment editor and analysis program for Windows 95/98/ NT. Nucleic Acids Symp. 10.14601/Phytopathol_Mediterr-14998u1.29.

He B, Xu W, Santini PA, Polydorides AD, Chiu A, Estrella J, Shan M, Chadburn A, Villanacci V, Plebani A, et al. (2007). Intestinal bacteria trigger T cell-independent immunoglobulin A(2) class switching by inducing epithelial-cell secretion of the cytokine APRIL. Immunity 26, 812–826. [PubMed: 17570691]

Hothorn T, Hornik K, van de Wiel MA, and Zeileis A (2008). Implementing a Class of Permutation Tests: The coin Package. J. Stat. Softw 10.18637/jss.v028.i08.

Horns F, Vollmers C, Croote D, Mackey SF, Swan GE, Dekker CL, Davis MM, and Quake SR (2016). Lineage tracing of human B cells reveals the *in vivo* landscape of human antibody class switching. eLife 5, e16578. [PubMed: 27481325]

Horwitz JA, Bar-On Y, Lu CL, Fera D, Lockhart AAK, Lorenzi JCC, Nogueira L, Golijanin J, Scheid JF, Seaman MS, et al. (2017). Non-neutralizing antibodies alter the course of HIV-1 infection in vivo. Cell 170, 637–648.e10. [PubMed: 28757252]

Jabara CB, Jones CD, Roach J, Anderson JA, and Swanstrom R (2011). Accurate sampling and deep sequencing of the HIV-1 protease gene using a Primer ID. Proc. Natl. Acad. Sci. USA 108, 20166–20171. [PubMed: 22135472]

Jackson KJL, Wang Y, and Collins AM (2014). Human immunoglobulin classes and subclasses show variability in VDJ gene mutation levels. Immunol. Cell Biol 92, 729–733. [PubMed: 24913324]

Janda A, Bowen A, Greenspan NS, and Casadevall A (2016). Ig constant region effects on variable region structure and function. Front. Microbiol 7, 22. [PubMed: 26870003]

Jia M, Liberatore RA, Guo Y, Chan KW, Pan R, Lu H, Waltari E, Mittler E, Chandran K, Finzi A, et al. (2020). VSV-displayed HIV-1 envelope identifies broadly neutralizing antibodies class-switched to IgG and IgA. Cell Host Microbe 27, 963–975.e5. [PubMed: 32315598]

Kardava L, and Moir S (2019). B-cell abnormalities in HIV-1 infection: roles for IgG3 and T-bet. Curr. Opin. HIV AIDS 14, 240–245. [PubMed: 30973418]

Katoh K, and Standley DM (2013). MAFFT multiple sequence alignment software version 7: improvements in performance and usability. Mol. Biol. Evol 30, 772–780. [PubMed: 23329690]

Kawamoto S, Maruya M, Kato LM, Suda W, Atarashi K, Doi Y, Tsutsui Y, Qin H, Honda K, Okada T, et al. (2014). Foxp3+ T cells regulate immunoglobulin a selection and facilitate diversification of bacterial species responsible for immune homeostasis. Immunity 41, 152–165. [PubMed: 25017466]

Keele BF, Giorgi EE, Salazar-Gonzalez JF, Decker JM, Pham KT, Salazar MG, Sun C, Grayson T, Wang S, Li H, et al. (2008). Identification and characterization of transmitted and early founder virus envelopes in primary HIV-1 infection. Proc. Natl. Acad. Sci. USA 105, 7552–7557. [PubMed: 18490657]

Kitaura K, Yamashita H, Ayabe H, Shini T, Matsutani T, and Suzuki R (2017). Different somatic hypermutation levels among antibody subclasses disclosed by a new next-generation sequencing-based antibody repertoire analysis. Front. Immunol 8, 389. [PubMed: 28515723]

Knudsen NPH, Olsen A, Buonsanti C, Follmann F, Zhang Y, Coler RN, Fox CB, Meinke A, D'Óro U, Casini D, et al. (2016). Different human vaccine adjuvants promote distinct antigen-independent immunological signatures tailored to different pathogens. Sci. Rep 6, 19570. [PubMed: 26791076]

Kozel TR, Thorkildson P, Brandt S, Welch WH, Lovchik JA, AuCoin DP, Vilai J, and Lyons CR (2007). Protective and immunochemical activities of monoclonal antibodies reactive with the Bacillus anthracis polypeptide capsule. Infect. Immun 75, 152–163. [PubMed: 17060470]

Kulkarni V, and Ruprecht RM (2017). Mucosal IgA responses: damaged in established HIV infection-yet, effective weapon against HIV transmission. Front. Immunol 8, 1581. [PubMed: 29176985]

Kwong PD, and Mascola JR (2018). HIV-1 vaccines based on antibody identification, B cell ontogeny, and epitope structure. Immunity 48, 855–871. [PubMed: 29768174]

Larkin MA, Blackshields G, Brown NP, Chenna R, McGettigan PA, McWilliam H, Valentin F, Wallace IM, Wilm A, Lopez R, et al. (2007). Clustal W and Clustal X version 2.0. Bioinformatics 23, 2947–2948. [PubMed: 17846036]

Li M, Gao F, Mascola JR, Stamatatos L, Polonis VR, Koutsoukos M, Voss G, Goepfert P, Gilbert P, Greene KM, et al. (2005). Human immunodeficiency virus type 1 env clones from acute and early subtype B infections for standardized assessments of vaccine-elicited neutralizing antibodies. J. Virol 79, 10108–10125. [PubMed: 16051804]

Li S, Lefranc MP, Miles JJ, Alamyar E, Giudicelli V, Duroux P, Freeman JD, Corbin VDA, Scheerlinck JP, Frohman MA, et al. (2013). IMGT/HighV QUEST paradigm for T cell receptor IMGT clonotype diversity and next generation repertoire immunoprofiling. Nat. Commun 4, 2333. [PubMed: 23995877]

Liao HX, Lynch R, Zhou T, Gao F, Alam SM, Boyd SD, Fire AZ, Roskin KM, Schramm CA, Zhang Z, et al.; NISC Comparative Sequencing Program (2013). Co-evolution of a broadly neutralizing HIV-1 antibody and founder virus. Nature 496, 469–476. [PubMed: 23552890]

Lindner C, Thomsen I, Wahl B, Ugur M, Sethi MK, Friedrichsen M, Smoczek A, Ott S, Baumann U, Suerbaum S, et al. (2015). Diversification of memory B cells drives the continuous adaptation of secretory antibodies to gut microbiota. Nat. Immunol 16, 880–888. [PubMed: 26147688]

Magri G, Comerma L, Pybus M, Sintes J, Lligé D, Segura-Garzón D, Bascones S, Yeste A, Grasset EK, Gutzeit C, et al. (2017). Human secretory IgM emerges from plasma cells clonally related to gut memory B cells and targets highly diverse commensals. Immunity 47, 118–134.e8. [PubMed: 28709802]

Maurer MA, Meyer L, Bianchi M, Turner HL, Le NPL, Steck M, Wyrzucki A, Orlowski V, Ward AB, Crispin M, and Hangartner L (2018). Glycosylation of human IgA directly inhibits influenza A and other sialic-acid-binding viruses. Cell Rep. 23, 90–99. [PubMed: 29617676]

Miranda LR, Duval M, Doherty H, Seaman MS, Posner MR, and Cavacini LA (2007). The neutralization properties of a HIV-specific antibody are markedly altered by glycosylation events outside the antigen-binding domain. J. Immunol 178, 7132–7138. [PubMed: 17513762]

Montefiori DC (2005). Evaluating neutralizing antibodies against HIV, SIV, and SHIV in luciferase reporter gene assays. Curr. Protoc. Immunol *Chapter 12*, Unit 12.11.

Moore PL, Ranchobe N, Lambson BE, Gray ES, Cave E, Abrahams MR, Bandawe G, Mlisana K, Abdool Karim SS, Williamson C, and Morris LCAPRISA 002 Study; NIAID Center for HIV/AIDS Vaccine Immunology (CHAVI) (2009). Limited neutralizing antibody specificities drive neutralization escape in early HIV-1 subtype C infection. PLoS Pathog. 5, e1000598. [PubMed: 19763271]

Neidich SD, Fong Y, Li SS, Geraghty DE, Williamson BD, Young WC, Goodman D, Seaton KE, Shen X, Sawant S, et al.; HVTN 505 Team (2019). Antibody Fc effector functions and IgG3 associate with decreased HIV-1 risk. J. Clin. Invest 129, 4838–4849. [PubMed: 31589165]

Pappas L, Foglierini M, Piccoli L, Kallewaard NL, Turrini F, Silacci C, Fernandez-Rodriguez B, Agatic G, Giacchetto-Sasselli I, Pellicciotta G, et al. (2014). Rapid development of broadly influenza neutralizing antibodies through redundant mutations. Nature 516, 418–422. [PubMed: 25296253]

Petrova VN, Muir L, McKay PF, Vassiliou GS, Smith KGC, Lyons PA, Russell CA, Anderson CA, Kellam P, and Bashford-Rogers RJM (2018). Combined influence of B-cell receptor

rearrangement and somatic hypermutation on B-cell class-switch fate in health and in chronic lymphocytic leukemia. Front. Immunol 9, 1784. [PubMed: 30147686]

Planer JD, Peng Y, Kau AL, Blanton LV, Ndao IM, Tarr PI, Warner BB, and Gordon JI (2016). Development of the gut microbiota and mucosal IgA responses in twins and gnotobiotic mice. Nature 534, 263–266. [PubMed: 27279225]

Pollara J, Bonsignori M, Moody MA, Liu P, Alam SM, Hwang K-K, Gurley TC, Kozink DM, Armand LC, Marshall DJ, et al. (2014). HIV-1 vaccine-induced C1 and V2 Env-specific antibodies synergize for increased antiviral activities. J. Virol 88, 7715–7726. [PubMed: 24807721]

Reed JH, Jackson J, Christ D, and Goodnow CC (2016). Clonal redemption of autoantibodies by somatic hypermutation away from self-reactivity during human immunization. J. Exp. Med 213, 1255–1265. [PubMed: 27298445]

Richardson SI, Chung AW, Natarajan H, Mabvakure B, Mkhize NN, Garrett N, Abdool Karim S, Moore PL, Ackerman ME, Alter G, and Morris L (2018). HIV-specific Fc effector function early in infection predicts the development of broadly neutralizing antibodies. PLoS Pathog. 14, e1006987. [PubMed: 29630668]

Richardson SI, Lambson BE, Crowley AR, Bashirova A, Scheepers C, Garrett N, Abdool Karim S, Mkhize NN, Carrington M, Ackerman ME, et al. (2019). IgG3 enhances neutralization potency and Fc effector function of an HIV V2-specific broadly neutralizing antibody. PLoS Pathog. 15, e1008064. [PubMed: 31841557]

Sabouri Z, Schofield P, Horikawa K, Spierings E, Kipling D, Randall KL, Langley D, Roome B, Vazquez-Lombardi R, Rouet R, et al. (2014). Redemption of autoantibodies on anergic B cells by variable-region glycosylation and mutation away from self-reactivity. Proc. Natl. Acad. Sci. USA 111, E2567–E2575. [PubMed: 24821781]

Sacks D, Bhiman JN, Wiehe K, Gorman J, Kwong PD, Morris L, and Moore PL (2019). Somatic hypermutation to counter a globally rare viral immunotype drove off-track antibodies in the CAP256-VRC26 HIV-1 V2-directed bNAb lineage. PLoS Pathog. 15, e1008005. [PubMed: 31479499]

Scheepers C, Shrestha RK, Lambson BE, Jackson KJL, Wright IA, Naicker D, Goosen M, Berrie L, Ismail A, Garrett N, et al. (2015). Ability to develop broadly neutralizing HIV-1 antibodies is not restricted by the germline Ig gene repertoire. J. Immunol 194, 4371–4378. [PubMed: 25825450]

Schramm CA, Sheng Z, Zhang Z, Mascola JR, Kwong PD, and Shapiro L (2016). SONAR: A high-throughput pipeline for inferring antibody ontogenies from longitudinal sequencing of B cell transcripts. Front. Immunol 7, 372. [PubMed: 27708645]

Schroeder HWJ Jr., and Cavacini L (2010). Structure and function of immunoglobulins. J. Allergy Clin. Immunol 125 (2, Suppl 2), S41–S52. [PubMed: 20176268]

Soto C, Ofek G, Joyce MG, Zhang B, McKee K, Longo NS, Yang Y, Huang J, Parks R, Eudailey J, et al.; NISC Comparative Sequencing Program (2016). Developmental pathway of the MPER-directed HIV-1-neutralizing antibody 10E8. PLoS ONE 11, e0157409. [PubMed: 27299673]

Stern JNH, Yaari G, Vander Heiden JA, Church G, Donahue WF, Hintzen RQ, Huttner AJ, Laman JD, Nagra RM, Nylander A, et al. (2014). B cells populating the multiple sclerosis brain mature in the draining cervical lymph nodes. Sci. Transl. Med 6, 248ra107.

Tudor D, Yu H, Maupetit J, Drillet AS, Bouceba T, Schwartz-Cornil I, Lopalco L, Tuffery P, and Bomsel M (2012). Isotype modulates epitope specificity, affinity, and antiviral activities of anti-HIV-1 human broadly neutralizing 2F5 antibody. Proc. Natl. Acad. Sci. USA 109, 12680–12685. [PubMed: 22723360]

van Loggerenberg F, Mlisana K, Williamson C, Auld SC, Morris L, Gray CM, Abdool Karim Q, Grobler A, Barnabas N, Iriogbe I, and Abdool Karim SS; CAPRISA 002 Acute Infection Study Team (2008). Establishing a cohort at high risk of HIV infection in South Africa: challenges and experiences of the CAPRISA 002 acute infection study. PLoS ONE 3, e1954. [PubMed: 18414658]

Victora GD, and Nussenzweig MC (2012). Germinal centers. Annu. Rev. Immunol 30, 429–457. [PubMed: 22224772]

Vidarsson G, Dekkers G, and Rispens T (2014). IgG subclasses and allotypes: from structure to effector functions. Front. Immunol 5, 520. [PubMed: 25368619]

Woof JM, and Mestecky J (2005). Mucosal immunoglobulins. Immunol. Rev 206, 64–82. [PubMed: 16048542]

Woof JM, and Russell MW (2011). Structure and function relationships in IgA. Mucosal Immunol. 4, 590–597. [PubMed: 21937984]

Wu X, Zhang Z, Schramm CA, Joyce MG, Kwon YD, Zhou T, Sheng Z, Zhang B, O'Dell S, McKee K, et al.; NISC Comparative Sequencing Program (2015). Maturation and diversity of the VRC01-antibody lineage over 15 years of chronic HIV-1 infection. Cell 161, 470–485. [PubMed: 25865483]

Yates NL, Lucas JT, Nolen TL, Vandergrift NA, Soderberg KA, Seaton KE, Denny TN, Haynes BF, Cohen MS, and Tomaras GD (2011). Multiple HIV-1-specific IgG3 responses decline during acute HIV-1: implications for detection of incident HIV infection. AIDS 25, 2089–2097. [PubMed: 21832938]

Zhang J, Kobert K, Flouri T, and Stamatakis A (2014). PEAR: a fast and accurate Illumina Paired-End reAd mergeR. Bioinformatics 30, 614–620. [PubMed: 24142950]

Zhou S, Jones C, Mieczkowski P, and Swanstrom R (2015). Primer ID validates template sampling depth and greatly reduces the error rate of Next-Generation Sequencing of HIV-1 genomic RNA populations. J. Virol 89, 8540–8555. [PubMed: 26041299]

Highlights

- Multiple co-circulating isotypes within an HIV neutralizing antibody lineage
- Differential neutralization of emerging viral escape variants is mediated by isotype
- Detrimental isotype switching can be rescued by further class-switch recombination
- Class-switch recombination contributes to antibody-virus co-evolution

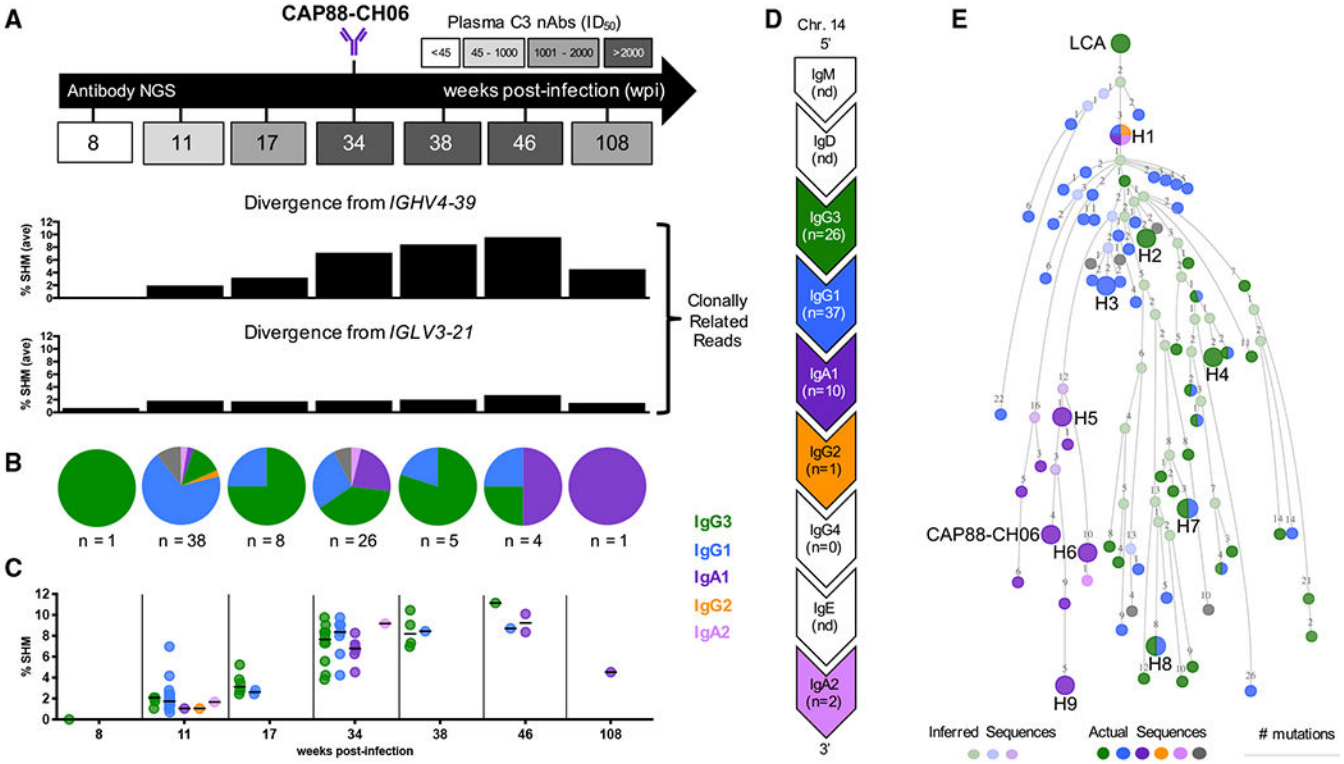

Figure 1. The CAP88-CH06 Antibody Lineage Comprises Multiple Co-evolving Isotypes

(A) Longitudinal antibody NGS spanning the appearance and waning of C3-directed neutralizing antibodies in donor CAP88. Each box indicates the time point in weeks post-infection (wpi) when antibody NGS was performed and is gray-scaled based on the C3-specific plasma-neutralizing antibody titer (Moore et al., 2009). The time point at which the CAP88-CH06 monoclonal antibody was previously isolated (Gray et al., 2011) is indicated. The average levels of heavy and light chain SHM in clonally related sequences, compared with their germline genes (*IGHV4-39* and *IGLV3-21*), are shown in the middle and bottom panels, respectively.

(B) Prevalence of CAP88-CH06 isotypes over 2 years of infection. Pie charts indicate the numbers of different isotypes observed at various time points, colored according to the isotype (gray denotes cases in which the IgG subtype could not be assigned because of similarities in the primer region).

(C) Levels of SHM over time, by isotype, within the heavy-chain variable regions for each clonally related sequence.

(D) Relative location of isotype-specific *IGHC* genes on chromosome 14, defining the direction in which CSR occurs. The numbers of sequences observed for each isotype is shown, nd, not done.

(E) Antibody-lineage reconstruction with sequences colored by isotype. Sequences inferred by Change-O, part of the immcantation portal, are indicated as translucent symbols, whereas filled symbols indicate nodes observed in NGS sequences. The number of mutations between nodes is shown as integers, and line lengths between nodes are proportional to those. Nodes indicating the LCA, the mature CAP88-CH06 sequence, and several heavy-

chain sequences used for downstream analyses (H1–H9) are enlarged and labeled on the tree. H5-IgA1 was observed both at 34 and 108 wpi.
See also Figures S1 and S2 and Table S1.

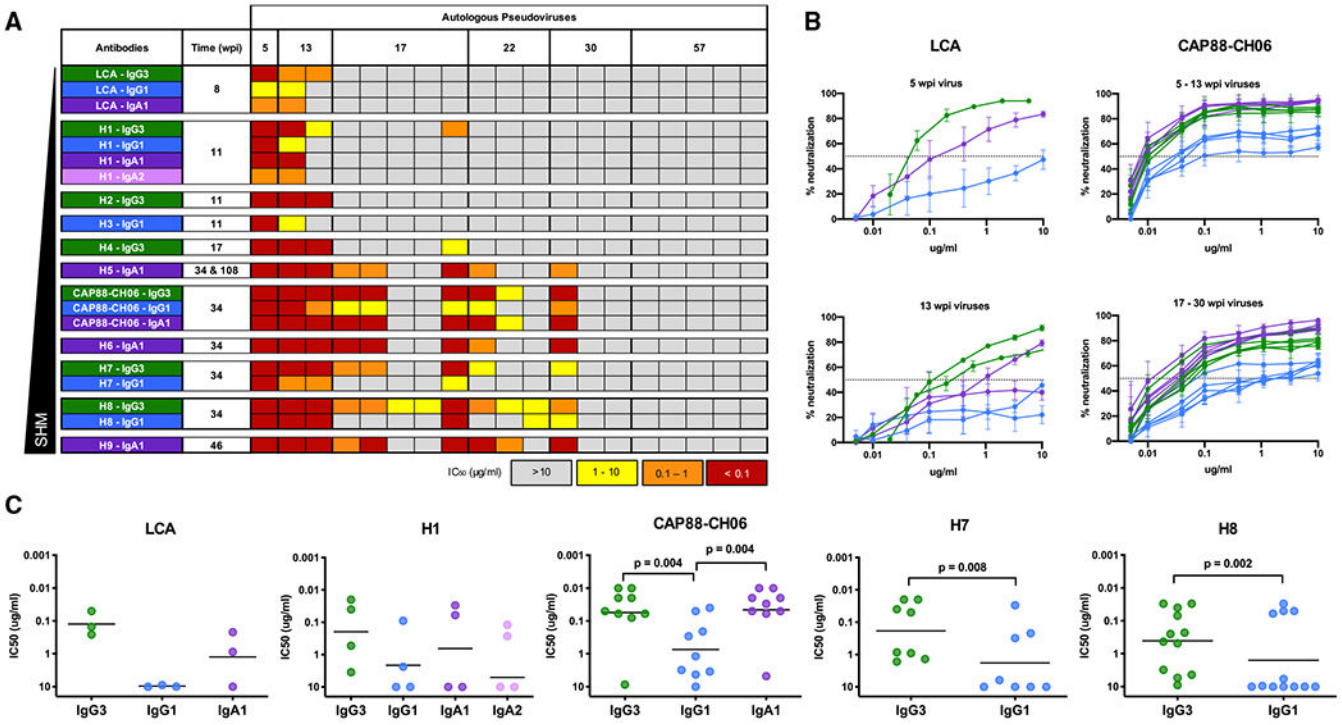

Figure 2. Potent Neutralization of Autologous Viruses by IgG3 and IgA1 Isotypes of CAP88-CH06

(A) Neutralization of the CAP88 T/F virus (5 wpi) and longitudinal viral Env clones isolated up to 57 wpi (when complete viral escape occurred) by the LCA, H1–H9, and the mature CAP88-CH06 mAbs, colored by isotype. Data are shown as a heatmap of neutralization titers (half-maximal inhibitor concentration [IC_{50}]); no neutralization at 10 μg/mL (gray), neutralization between 1 and 10 μg/mL (yellow), 0.1 and 1 μg/mL (orange), and neutralization less than 0.1 μg/mL (red).

(B) Neutralization curves against autologous viruses for the LCA (left panel) and for CAP88-CH06 (right panel) expressed as different isotypes (IgG3, green; IgG1, blue; and IgA1, purple). The dotted line in the graphs represents IC_{50}. Error bars represent standard deviations.

(C) Comparison of neutralization potency for all antibodies with identical variable regions but different isotypes against autologous viruses from 5 to 57 wpi. The mAbs are colored by isotype in order of CSR (IgG3, green; IgG1, blue; IgA1, purple; and IgA2, pink). Geometric mean of potency for each antibody is shown by a solid line. Statistically significant differences among isotypes were assessed with a Wilcoxon signed-rank test, denoted by p values, and had large effect sizes of 0.63, 0.63, 0.67, and 0.56 with Z scores of 2.6, 2.6, 2.5, and 2.9, respectively.

See also Figure S3.

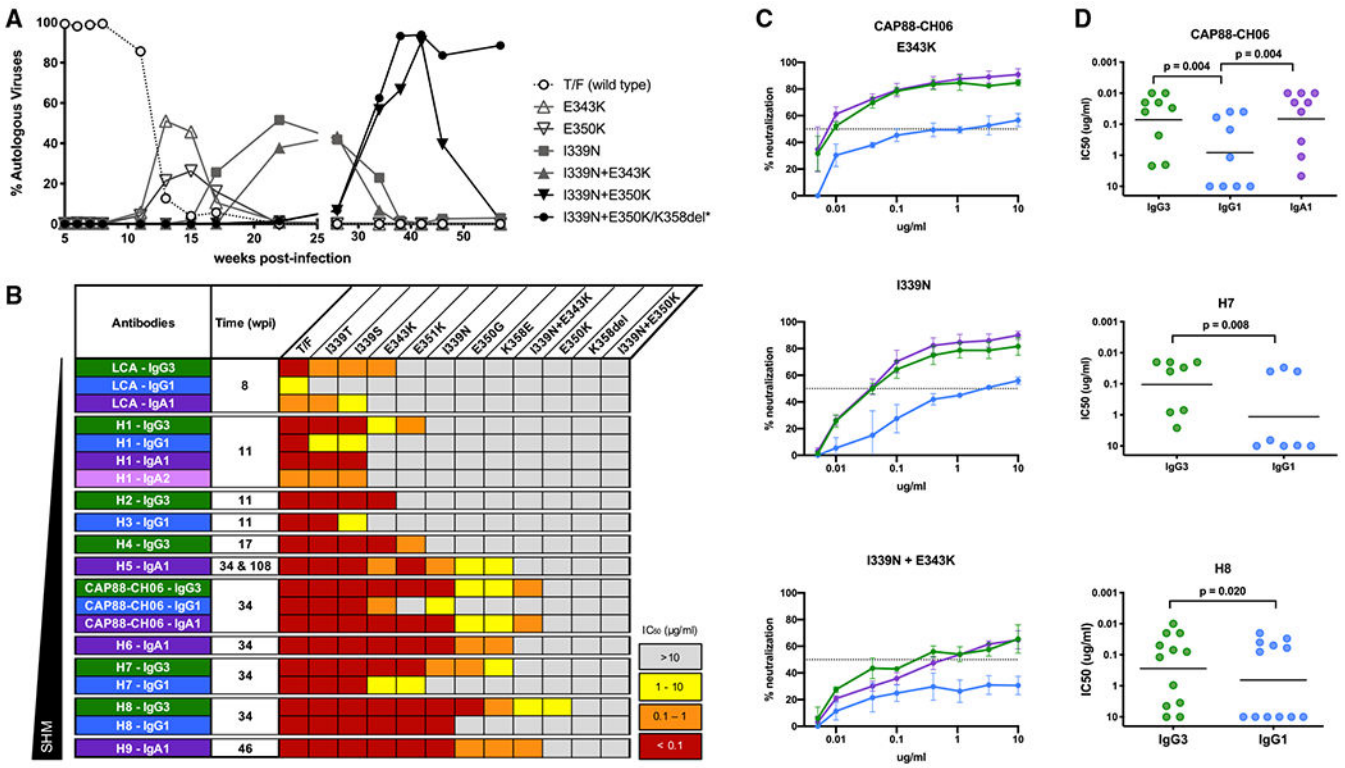

Figure 3. CAP88-CH06 as IgG1 Shows Reduced Neutralization of Viral Escape Variants Compared with IgG3 and IgA1

(A) Longitudinal kinetics of dominant CAP88 viral escape mutations, individually and in combination, from 5 to 57 wpi. Shown are the relative frequencies (percentage of autologous viruses) of each escape mutation over time (wpi) based on deep sequencing of the C3 region of the viral envelope (Table S2). The dotted line denotes the T/F virus. The combination of I339N and E350K or K358del, with or without other mutation(s), is denoted by I339N +E350K/K358del*.

(B) Neutralization titers against the T/F virus mutated to contain key escape mutations. Data are shown as a heatmap of neutralization titers (IC_{50}); no neutralization at 10 μg/mL (gray), neutralization between 1 and 10 μg/mL (yellow), 0.1–1 μg/mL (orange), and less than 0.1 μg/mL (red). Viral escape mutations are ordered by degree of neutralization resistance.

(C) Neutralization curves of CAP88-CH06 expressed as different isotypes (IgG3, green; IgG1, blue; and IgA1, purple) against viruses bearing the E343K, I339N, and I339N+E343K mutations. The dotted line in the graphs represents IC_{50}. Error bars represent standard deviations.

(D) Comparison of neutralization potency for CAP88-CH06, H7, and H8 that showed statistically significant differences in titers between isotypes against viral escape mutants. Shown are the IC_{50} (μg/mL) for each mAb against the CAP88 T/F and sensitive viral escape mutants. The mAbs are colored according to isotype (as above). Geometric mean of potency for each antibody is shown by a solid line. Statistically significant differences among isotypes were determined with a Wilcoxon signed-rank test, denoted by p values, and had large effect sizes of 0.6, 0.6, 0.63, and 0.51 with *Z* scores of 2.7, 2.7, 2.5, and 2.3, respectively.

See also Tables S2 and S3.

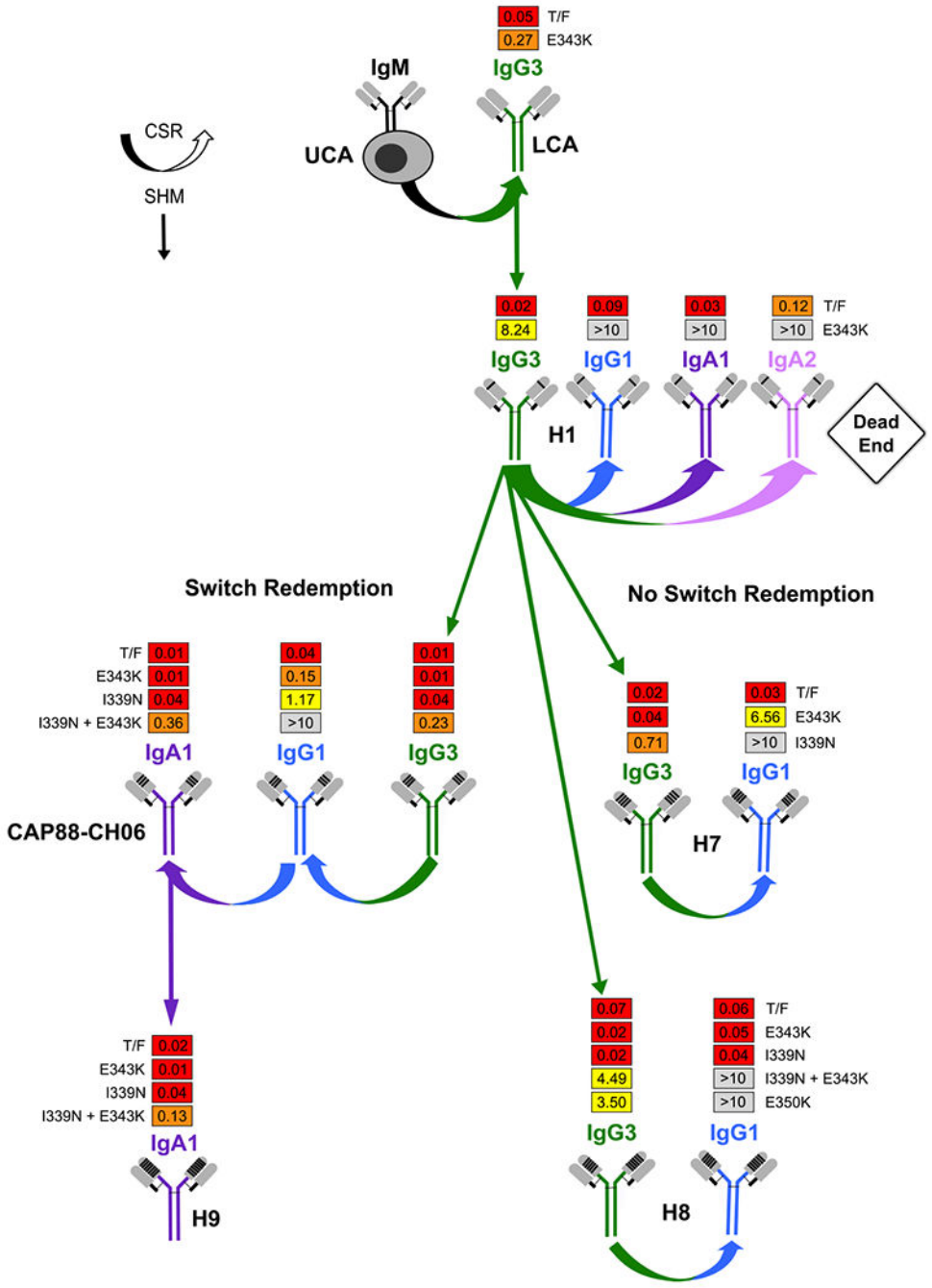

Figure 4. The Role of Class-Switch Recombination and Isotype in Antibody-Virus Co-evolution

Schematic diagram of the influence of isotype and SHM on antibody-virus co-evolution in donor CAP88. Curved horizontal arrows represent class-switch recombination (CSR) events and are colored to indicate isotypes being switched. Straight vertical arrows represent increases in SHM (also indicated schematically on antibodies as black lines within heavy-chain variable regions). IC_{50} neutralization titers for the T/F virus and selected escape mutations are shown above each antibody. Mutations are ranked in order of resistance, with E350K being the most resistant. Four examples (for H1, H7, H8, and CAP88-CH06) of

detrimental switches are shown, where a switch from IgG3 to another isotype, usually IgG1, results in reduced neutralization. However, in CAP88-CH06, a further isotype switch from IgG1 to IgA1 rescued that loss of neutralization. See also Table S3.

KEY RESOURCES TABLE

REAGENT or RESOURCE	SOURCE	IDENTIFIER
Antibodies		
Palivizumab	Medimmune	Synagis; RRID: AB_2459638
A32	NIH AIDS Reagent Program	11438
CAP88-CH06	NICD	n/a
KC57-FITC p24 antibody	Beckman-Coulter	6604665
Bacterial and Virus Strains		
Escherichia coli JM109	Inqaba	T3003
Escherichia coli XL 10-Gold Ultracompetent Cells	Agilent Technologies	200315
Biological Samples		
CAP88-derived PBMC samples	CAPRISA (van Loggerenberg et al., 2008)	CAPRISA (https://www.caprisa.org)
CAP88-derived Plasma samples	CAPRISA (van Loggerenberg et al., 2008)	CAPRISA (https://www.caprisa.org)
Pooled HIV Clade C IgG	NIH AIDS Reagent Program	3957
HIV negative donor PBMC	NICD	N/A
Chemicals, Peptides, and Recombinant Proteins		
Superscript III Reverse Transcriptase	Invitrogen	18080093
PfuUltra II Fusion HS DNA polymerase	Agilent	600380
X-tremeGene 9 DNA Transfection Reagent	Roche	06365809001
Ampure XP Beads	Beckman-Coulter	A63880
SPIRselect Magnetic Beads	Beckman-Coulter	B23317
FreeStyle 293 Expression Medium	LTC Tech SA	11625019
Protein A-Agarose	BioVision	6526-100
Immobilized Protein G	ThermoFischer Scientific	20397
CaptureSelect™ IgA Affinity Matrix	ThermoFischer Scientific	194288010
PhiX Control V3	Illumina	FC-110-3001
Critical Commercial Assays		
QiAamp Viral RNA kit	QIAGEN	52904
AllPrep DNA/RNA mini kit	QIAGEN	80204
Nextera XT Indexing Kit V2 Set B (Antibody NGS)	Illumina	FC-131-2002
Nextera XT Indexing Kit V2 Set A (Viral NGS)	Illumina	FC-131-2001

REAGENT or RESOURCE	SOURCE	IDENTIFIER
Big Dye™ Terminator v3.1 Cycle Sequencing Kit	Applied Biosystems	4337456
MiSeq Reagent Kit V3	Illumina	MS-102-3003
Qubit dsDNA HS assay	ThermoFischer Scientific	Q32854
Agilent High Sensitivity DNA Kit	Agilent Technologies	5067-4626
Deposited Data		
Raw Antibody MiSeq Data	This paper (SRA)	SRA:PRJNA556126
Lineage Antibody Sequences	This paper (GenBank)	GenBank:MN228641 - GenBank:MN228657
Raw C3 Envelope MiSeq Data	This paper (SRA)	SRA:PRJNA557574
Single Genome Amplification Env Sequences	This paper (GenBank)	GenBank:KU198436.1, GenBank:MK205449.1, GenBank:MK205458.1, GenBank:MK205486.1, GenBank:MK205487.1, GenBank:MK205490.1, GenBank:MK205492.1, GenBank:MK205495.1, GenBank:MK205508.1, GenBank:MK205514.1L, GenBank:MK205520.1, GenBank:MK205531.1, GenBank:MK205564.1, GenBank:MK205575.1, GenBank:MK206069.1, GenBank:MK206074.1, GenBank:MK206078.1, GenBank:MK206112.1 and GenBank:MK206156.1
Experimental Models: Cell Lines		
HEK293F	LTC Tech SA	11625019
HEK293T	Dr George Shaw	University of Alabama
CEM.NK$^{R}_{CCR5}$	NIH AIDS Research Reagent Program	4376
TZM-bl	NIH AIDS Research Reagent Program	8129
Oligonucleotides		
EnvM primer: 5′-TAGCCCTTCCAGTCCCCCCTTTTCTTTTA-3′	Gao et al., 1996	N/A
EnvA primer: 5′-GGCTTAGGCATCTCCTATGGCAGGAAGAA-3′	Gao et al., 1996	N/A
IGHV4-39 forward primer: 5′-TCGTCGGCAGCGTCAGATGTGTATAAGAGACAGCAGSTGCAGCTGCAGGAGTCGG-3′	Integrated DNA Technologies	N/A
IGLV3-21 forward primer: 5′-TCGTCGGCAGCGTCAGATGTGTATAAGAGACAGTCCTATGTGCTGACTCAGCCACCC-3′	Integrated DNA Technologies	N/A

REAGENT or RESOURCE	SOURCE	IDENTIFIER
IgG reverse primer: 5′-GTCTCGTGGGCTCGGAGATGTGTATAAGAGACAGGCTTGACCAGGCAGCCCAGGGC-3′	Integrated DNA Technologies	N/A
IgA reverse primer: 5′-GTCTCGTGGGCTCGGAGATGTGTATAAGAGACAGGAAGAAGCCCTGGACCAGGCA-3′	Integrated DNA Technologies	N/A
Lambda reverse primer: 5′-GTCTCGTGGGCTCGGAGATGTGTATAAGAGACAGGCACCAGTGTGGCCTTGTTGGCTTG-3′	Integrated DNA Technologies	N/A
ENV_C3_cDNA_R: 5′-GCCTTGCCACACGCTCAGGCNNNNNNNNNNNNNNNTGTGTTGTAAYTTCTAGRTC-3′	Integrated DNA Technologies	N/A
ENV_C2_Fwd,5′-TCGTCGGCAGCGTCAGATGTGTATAAGAGACAGNNNNNNNGCTGGTTATGCGATTCTAAAGTG-3′	Integrated DNA Technologies	N/A
Univ_i7_Rev,5′-GTCTCGTGGGCTCGGAGATGTGTATAAGAGACAGGCCTTGCCACACGCTCACGC-3′	Integrated DNA Technologies	N/A
Random Hexamers	Integrated DNA Technologies	51-0118-01
Recombinant DNA		
pCDNA 3.1D-TOPO	Invitrogen	K4900-01
$pSG3^{\Delta Env}$	NIH AIDS Reagent	11051
Software and Algorithms		
Sequencher v5.4.6	Genecodes	http://www.genecodes.com/
Clustal X v1.83	Larkin et al., 2007	http://www.clustal.org/
BioEdit v7.2.5	Hall, 1999	https://bioedit.software.informer.com/7.2/
SONAR	Schramm et al., 2016	https://github.com/scharch/SONAR and https://hub.docker.com/r/scharch/sonar/
PEAR v0.9.6	Zhang et al., 2014	https://cme.h-its.org/exelixis/web/software/pear/
USEARCH v9.0.2132	Edgar, 2010	http://www.drive5.com/usearch
R v3.5.3		https://www.r-project.org/
R coin package	Hothorn et al., 2008	https://cran.r-project.org/web/packages/coin/index.html
R igraph package	Csardi and Nepusz, 2006	https://igraph.org/r/
R alakazam package	Stern et al., 2014	https://cran.r-project.org/web/packages/alakazam/index.html
Immcantation portal	Gupta et al., 2015	https://immcantation.readthedocs.io/en/stable
IMGT High V-Quest	Alamyar et al., 2012	http://www.imgt.org/HighV-QUEST/home.action

REAGENT or RESOURCE	SOURCE	IDENTIFIER
NGS Data Processing Pipeline	HIV Diversity Group, UCT	https://github.com/HIVDiversity/NGS_processing_pipeline
MotifBinner2	HIV Diversity Group, UCT	https://github.com/HIVDiversity/MotifBinner2
MAFFT v7.427	Katoh and Standley, 2013	https://mafft.cbrc.jp/alignment/software/
Python scripts for viral aa frequencies	HIV Diversity Group, UCT	https://github.com/HIVDiversity/NGS_analysis_pipeline/blob/master/calc_multi_site_freq.py